Grain Refinement Tracing of Dynamic and Metadynamic Recrystallization for a Penetrator Steel

Taher El-Bitar[1], Maha El-Meligy[1], Wojciech Borek[2], Saad Ebied[3]*

[1]Plastic Deformation Dept., Central Metallurgical R&D Institute (CMRDI), 1st El-Felazaat St., Eltabeen, 11722 Helwan, Egypt;
[2]Department of Engineering Materials and Biomaterials, Silesian University of Technology, 18A Konarskiego Street, 44-100 Gliwice, Poland;
[3]Production Engineering and Mechanical Design Department, Faculty of Engineering - Tanta University, Tanta 31527, Egypt.

**Corresponding author email: dr.mahaelmeligy@gmail.com*

ABSTRACT

The present investigation is dealing with the evolution of simultaneous dynamic and metadynamic recrystallization (DRX)& (MDRX) phenomena by physical simulation for a 4-strock hot compression process, where flow curves were presented for each stroke. The primary alloy is a penetrator steel containing 0.3% C in addition to some Cr, Mo, Ni and 1.63 W. Calculated grain size after the onest of DRX & occurrence of MDRX decreases continuously with the increase of cumulative strain reaching to 0.289 µm. However, Electron Backscatter Diffraction (EBSD) investigation established that 99% of the grains, after the last compression stroke, were detected as <1.0 µm, with an average grain size 0.31 µm. Microstructure after simulation presents fine lath martensitic structure, coexisting with Cr-W carbides, which are crammed at the inter- martensite laths. Furthermore, 56% of the grains showed grain boundaries misorientation creating High Angle Grain Boundaries (HAGB), which are promoting MDRX. The flow curve of each stroke definitely contains two complementary microstructure events, namely a DRX, and a MDRX phenomenon, where the peak stress (σ_p) of DRX is inversely proportional to the mean temperature of stroke.

Keywords: Hot Compression Simulation, Dynamic and Metadynamic Recrystallization, Electron Backscatter Diffraction (EBSD), HAGB& LAGB, Grain Refinement, Penetrator Steel.

1. Introduction

Metallic materials with uniform ultra-fine-grained microstructures are characterized by beneficial combination of their mechanical properties. Such metals and alloys demonstrate high strength, which is combined by improved impact toughness with sufficient ductility. Dynamic recrystallization (DRX) is one of the most important mechanisms for microstructure evolution during deformation. DRX occurs during straining of metals at high temperature, characterized by a nucleation of low dislocation density grains and a subsequent growth that can produce a homogeneous grain size when equilibrium is reached. DRX is able to cause a great impact on the hot flow behavior, affecting the microstructure and properties of the material after processing, where the desired mechanical properties can be achieved by acting on the DRX kinetics [1]. Frequently, the presence of DRX is indicated by a well-defined peak stress value (σ_p) on the true stress–true strain (σ_t–ε_t) curves.

DRX is usually initiated before the strain corresponding to σ_p. It is reported that this particular value of strain is linked with the minimum amount of stored energy induced by deformation needed to start DRX [2, 3] and is defined as the critical strain (ε_c) for the onset of DRX, associated with the critical stress (σ_c). Generally, this critical value is related to the nucleation by the formation of mobile high angle grain boundaries (HAGB) simultaneously

with the strain conditions.

When the critical strain is reached, DRX would be created where the grain becomes saturated of dislocation barriers that forming cells and the grain boundaries bulge until a new grain is formed. Upon the peak stress, (σ_p), the stress descends following a particular kinetic rate until arriving to the steady state stress, σ_{ss} [1,4]. Detailed study was investigated for evolution of microstructure during hot deformation. Verlinden et al. [5], insured DRX happening after a peak on the flow curve and continue to a full dynamic recrystallization, with the existence of dynamic equilibrium. However, continuous dynamic recrystallization (CDRX) is accompanied with unavoidable simultaneous post dynamic recrystallization action [5].

Subgrain structures with low angle grain boundaries (LAGBs) are formed during deformation for materials with high SFE due to the efficient dynamic recovery, they progressively evolve into high angle grain boundaries (HAGBs) at larger deformations, a process which is known as continuous dynamic recrystallization (CDRX) [6].

The presence of the DRV promotes equilibrium and the rate of strain hardening (SH) progressively decreases with straining and becomes minima at high strains, leading to a steady state stress. This behavior appears and remains just after the maximum stress [7]. On the other hand, in low SFE materials such as gamma-iron austenite (γ-Fe), the DRV kinetics is slow, allowing DRX to take place because the large amount of dislocations generated during work hardening is not annihilated. Therefore, it can be assumed that, once a certain critical dislocation density value ρ_c (associated to a critical strain) is reached, DRX is activated as an additional softening mechanism [7].

During deformation at the specific conditions, a peak is created at the flow curve summing up initiation of dynamic recrystallization (DRX) at a critical level of stress accumulation corresponding to a critical strain value [3]. DRX occurs easily with the increase of deformation temperature and decrease in strain rate. These conditions support DRX by increasing the mobility of grain boundaries and providing longer time for dislocation annihilation creating DRX [5].

The critical dislocation density depends on the strain rate, temperature, chemical composition, and grain size. Under low strain rate conditions, and when the critical density value is attained, DRX is initiated mainly by the bulging of pre-existing grain boundaries. In the case of high strain rates, DRX is initiated by the growth of high angle boundaries (HAB) formed by dislocation accumulation [8].

For a single peak behavior, nucleation mainly occurs along existing grain boundaries, and the growth of each grain is stopped by the concurrent deformation. When all the grain boundary sites are occupied and exhausted, further new grains are nucleated within the primary grains at the interface of the recrystallized and un-recrystallized grains [9].

By time, deformation strains increase and two simultaneous microstructure events are working. The 1st one is the DRX, which was begun at the time of peak formation, while the 2nd event is a MDRX, which was referred earlier as post dynamic recrystallization [5], and created due to specific conditions. Furthermore, Once the DRX is initiated during the deformation, the DRX nuclei continue to grow even after the deformation is interrupted. This mechanism is identified as MDRX. MDRX apparently does not require an incubation time, because it makes use of the nuclei formed by DRX [10].

The initial grain size has a pronounced effect on the DRX kinetics and microstructure owing to the changes in the grain-boundary surface area conditions, thus affecting the nucleation kinetics. The finer initial grain size of the microstructure, the lower the critical and peak strains. Dislocations can accumulate more rapidly in a microstructure having a minor grain size; therefore, a higher specific grain boundary area–volume ratio promotes faster DRX kinetics affecting the microstructural and mechanical properties of the deformed structure [10-12]. Grain refinement can also result in a decrease of the ductile-to-brittle transition temperature (DBTT). DBTT = A − Kd$^{-1/2}$, where A and K are constants, and d is the mean grain size. Therefore, it is possible to find ways to promote ultra-fine grained (UFG) steels, which can improve the strength-to-weight ratio (specific strength) [13-15].

The critical strain (ε_c) of DRX is early onset with a decrease in the prior grain size, a decrease in strain rate, and with a temperature increase [10, 11].

An investigation for hot compression testing [16] revealed that dynamic recrystallisation started at a fraction of approximately 0.8 of the peak strain, originated by local bulging of grain boundaries.

It has been well known that finer initial grains can enhance DRX and lead to finer DRX grains. As a simplified description of the grain size at the peak (d_{peak}) can be expressed as [6]:

$$d_{peak} = d_o \cdot \exp\left(-\varepsilon_p\right) \quad\quad (1)$$

Where, d_{peak} is the grain size at peak point and initiation of DRX

d_o is the initial grain size before deformation. d_o in the present study is considered as 4.9 μm for the calculation of peak grain size in the 1st stroke [17].

ε_p is the peak strain at stroke. It may be attributed to the Metadynamic recrystallization (MDRX)

that takes place simultaneously with DRX [18], where MDRX occurs by continued growth of the nuclei formed by dynamic recrystallization during straining [19].

2. Material & Experimental work

The steel alloy was developed at CMRDI of Egypt, where the developed alloy contains 0.3% carbon in addition to 1.6 W. Detailed chemical composition as well as processing procedure were previously presented elsewhere [8]. The alloy was subjected to extensive cross-sectional reduction by forging from a rectangle with 100x35 mm to round bars with 15 mm diameter, i.e. 95% of area reduction [17]. The forged bars were machined to cylindrical specimens with dimensions 8.0 mm diameter and 11.0 mm height for use in the thermo-mechanical simulator (Gleeble 3800) to carryout 4-strokes hot compression for a possible successive dynamic recrystallization (DRX). Processing data at the simulator are presented and summarized in Fig. 1.

After the final simulation of the 4th stroke, the hot compressed specimens were directly water quenched to suppress the changes in grain size. True stress - true strain flow curves were comparatively presented for each deformation stroke in Fig.2.

Optical microstructure as well as Scanning Electron microscopic (SEM) photos at high magnifications were used to detect grain size after forging. The electron back scatter diffraction (EBSD) was conducted within the SEM which is equipped with energy dispersion X-ray analysis (EDXA) cameras to establish the average grain size and orientation.

3. Results and discussions

The current steel alloy was subjected to multi-steps directional hot forging to 15 mm diameter round bars with 95% of cross-sectional area reductions [8], which is leading to conditioning and grain refinement of the martensite [17] with 4.9 μm initial grain size (d_o) before simulation [17].

Fig. 3 presents SEM microstructures of the steel alloy after simulation of successive 4- strokes hot deformation. Fig. 3-a presents fine lath martensitic structure, however, in Fig. 3-b the photo is focusing on the Cr-W carbides, which are crammed at the inter- martensite laths [17, 20].

Table I summarizes different measured and calculated parameters for each stroke by using eq. 1 in addition to the calculations of the Z-parameter as:

$$Z\text{-parameter} = \varepsilon \cdot e^{Q/RT} \qquad (2)$$

Where ε is the strain rate. The activation energy for deformation (Q) is considered as 537 KJ/mole [21]. The final grain size after the Meta-dynamic recrystallization (d_{MDRX}) event can be expected by using the general formula:

$$d_{MDRX} = C\, Z^{-n} \qquad (3)$$

where, C & n are material constants.

MDRX grain sizes were calculated by using eq.3, where the most convenient and logical values of constants were statically investigated. Considering the constant C as 16.885×10^3 and n still equals -0.192 as proposed by ref. [22].

Fig.4 presents calculated grain size at the peak (d_{peak}) and MDRX grain size (d_{MDRX}) for each stroke of the simulation cycle. It is clear that the grain size during onset of DRX and MDRX events decrease with the increase of simulation stroke number (amount of strain). The comparative presentation
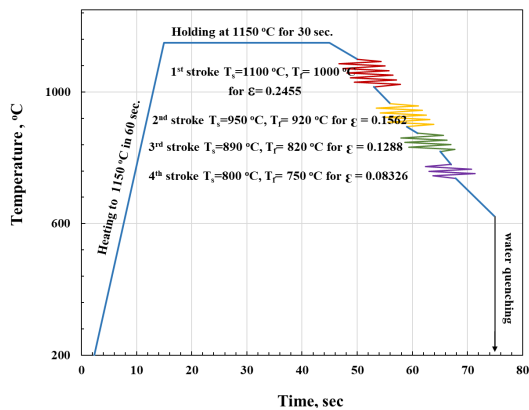
Fig. 1- 4-strokes of hot compressive cycles at the thermo-mechanical simulator (Gleeble 3800).
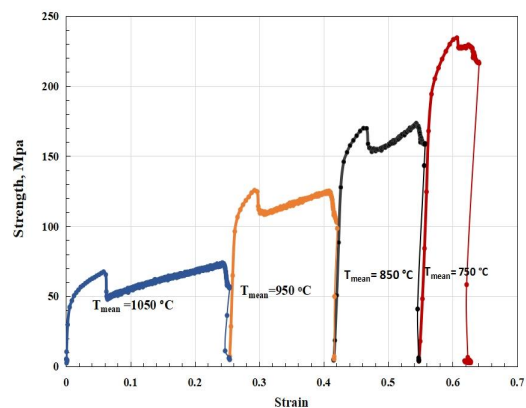
Fig. 2- A comparative presentation of the 4-strockes flow curves at mean processing temperatures 1050, 950, 850, and 750 °C.

clearly shows that grain refinement starts with the onset of DRX at peak on the flow curve and continued to ultra-fine structured of MDRX for promoting superior mechanical properties with a final MDRX grain size 0.289 μm.

Grain size measurement of the present work was done after deformation finish, which is directly followed by the water quenching. Here DRX &MDRX grains are coupled together [23]. Electron back scatter diffraction (EBSD) map (Fig .5) represents a combination of DRX & MDRX grains. Fig.5 is combined with a histogram grain size distribution after accumulated 4-strocke hot compressive cycle at the simulator. EBSD technique, with the aid of

energy dispersion X-ray analysis (EDXA) established that 99% of the recrystallized grains presented as < 1.0 μm average grain size. The mean grain size was statistically calculated as 0.31 μm with a standard deviation (STD) 0.16.

However, the calculated metadynamic recrystallize grain size value is 0.289 μm as was stated in Table I, which is near to that measured by the EBSD result.

The grain boundaries orientation of a cross-sectional area of the simulated samples were examined by EBSD technique. A grain mapping presented in Fig. 6 shows the relative orientation difference between neighboring grains. The grain mapping in-

Table 1- Calculated grain size at Peak strain and Metadynamic Grain size after deformation for each stroke

Parameter	Stroke temp.	Strain (ε)	Strain rate ($\dot{\varepsilon}$)	Peak strain (ε_p)	Grain size at peak strain (d_{peak})	Z-Parameter	Metadynamic Grain size (d_{MDRX})
units	K	---	Sec.$^{-1}$	----	μm	---	μm
1st stroke	1323	0.2455	0.0152	0.058	4.624	2.360E+19	3.220
2nd stroke	1208	0.1562	0.0303	0.039	3.097	4.909E+21	1.156
3rd stroke	1128	0.1288	0.0336	0.046	1.104	2.414E+23	0.547
4th stroke	1048	0.0833	0.0117	0.059	0.516	6.608E+24	0.289
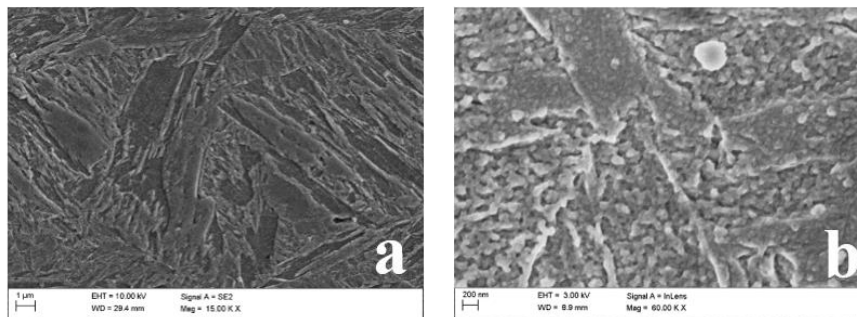
Fig. 3- SEM microstructures of the steel after simulation of 4- strokes hot deformation.
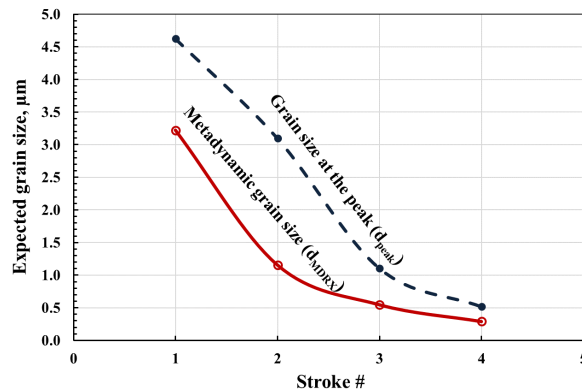
Fig. 4- Expected grain size at the peak strain and MDRX grain size (d_{peak} & d_{MDRX}) for each stroke of the simulation cycle.

sured that low angle grain boundaries (LAGB) and high angle grain boundaries (HAGB) are simultaneously happened by the action of grain misorientation. LAGB are drawn by green and red color lines, while HAGB are drawn by blue lines. LAGBs represent a considerable fraction of the grain boundaries (35.8%). These grains had an orientation difference (misorientation) equal or less than 15° relative to its neighboring grains. The total fraction of LAGB reflects high ability for promotion of dynamic softening creating DRX phenomena [24].

By time, during the simulation cycle deformation strains increase and two simultaneous microstructure events are created. The 1st one is the DRX, which was begun at the time of peak formation. The 2nd event is a MDRX, which is created due to specific conditions, where it was referred earlier as post dynamic recrystallization [5]. MDRX is then promoted by the action of misorientation of 64.2% of the total grain boundaries as HAGB [17]. Co-existing DRX and MDRX show strength increase with the increase of cumulative deformation strains and leading to a wonderful fine-grained structure [17], which is realizing superior mechanical prop-
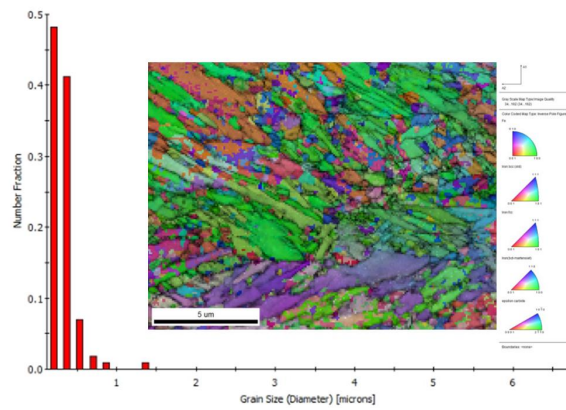
Fig. 5- Electron backscatter diffraction (EBSD) map and a histogram of grain size distrbuition.
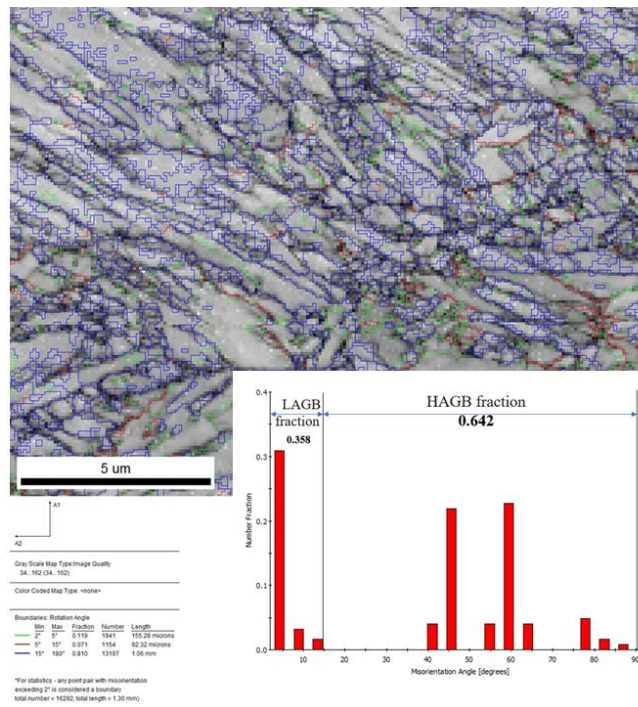
Fig. 6- EBSD map with misorientation angle distribution, indicating both low angle boundary grains (LABGs) and high angle boundary grains (HABGs).

erties [2].

Fig. 7 presents collective flow curves of successive 4-compression stroke simulation cycle. The onset of DRX is clearly featured by the peak on each flow curve, which is coupled together with MDRX [23], reflecting a strain hardening phenomena. Furthermore, each stroke is ended by softening phenomenon for a very short strain. Detailed stroke conditions are also reported on the figure for each flow curve in addition to the values of peak strain and stress.

Fig. 8 presents a relationship between the value of peak stress (σ_p) and the inverse of the stroke's temperature in Kelvin (1000/T). The linear trend observed in Fig. 8 indicates a proportional increase in peak stress (σp) with decreasing stroke temperature. This suggests a possible dominant role of temperature-dependent mechanisms on evolution of peak stress during deformation creating DRX and

MDRX events [25].

4.Conclusions

1- Grain size values after the onset of DRX and MDRX events decrease with the increase of simulation stroke number (amount of cumulative strain), where the final MDRX grain size is calculated as 0.289 μm.

2- EBSD technique established that the average grain size is statistically calculated as 0.31 μm, which conforms the calculated results.

3- MDRX is promoted by the action of 56% HAGBs, where the steel possesses strength increase with the increase of strain.

4 - Flow curve of each stroke contains two complementary microstructure events, namely DRX, and MDRX phenomenon.

5- Peak stress (σ_p) values are inversely proportional with the mean temperature of the strokes.

Fig. 7- A collective presentation of the 4-strocke compression flow curves.
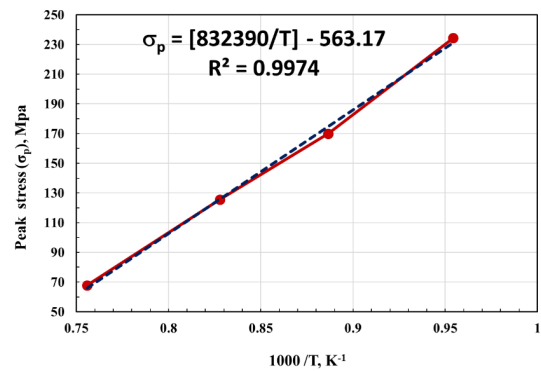
Fig. 8- A relationship between the peak stress (σ_p) value and 1000/stroke's temperature.

References

1. Jonas JJ. Dynamic recrystallization—scientific curiosity or industrial tool? Materials Science and Engineering: A. 1994;184(2):155-65.
2. Poliak EI, Jonas JJ. A one-parameter approach to determining the critical conditions for the initiation of dynamic recrystallization. Acta Materialia. 1996;44(1):127-36.
3. Alaneme KK, Okotete EA. Recrystallization mechanisms and microstructure development in emerging metallic materials: A review. Journal of Science: Advanced Materials and Devices. 2019;4(1):19-33.
4. Humphreys J, Hatherly M. Preface to the Second Edition. Recrystallization and Related Annealing Phenomena: Elsevier; 2004. p. xxvii.
5. Verlinden B, Driver J, Samadjar I, Doherty R.D, Softening mechanisms, in: Thermo-mechanical Processing of Metallic Materials, 2007; 11: 86-108.
6. Sakai T, Belyakov A, Kaibyshev R, Miura H, Jonas JJ. Dynamic and post-dynamic recrystallization under hot, cold and severe plastic deformation conditions. Progress in Materials Science. 2014;60:130-207.
7. Huang K, Logé RE. A review of dynamic recrystallization phenomena in metallic materials. Materials & Design.

2016;111:548-74.
8. El-Bitar T, ElMeligy M, Borek W, Ebied S. Characterization of Hot Deformation behavior for Ultra-High Strength (UHS) Steel containing Tungsten. Acta Metallurgica Slovaca. 2023;29(3):144-7.
9. Varela-Castro G, Cabrera J-M, Prado J-M. Critical Strain for Dynamic Recrystallization. The Particular Case of Steels. Metals. 2020;10(1):135.
10. Lenard JG, Pietrzyk M, Cser L. Introduction. Mathematical and Physical Simulation of the Properties of Hot Rolled Products: Elsevier; 1999. p. 1-10.
11. Derby B. The dependence of grain size on stress during dynamic recrystallisation. Acta Metallurgica et Materialia. 1991;39(5):955-62.
12. Galindo-Nava EI, Rivera-Díaz-del-Castillo PEJ. Grain size evolution during discontinuous dynamic recrystallization. Scripta Materialia. 2014;72-73:1-4.
13. Zhao L, Park N, Tian Y, Shibata A, Tsuji N. Combination of dynamic transformation and dynamic recrystallization for realizing ultrafine-grained steels with superior mechanical properties. Sci Rep. 2016;6:39127-.
14. Mintz B, Jonas JJ, Abu-shosha R. Effect of grain refinement and grain coarsening on shapes of dynamic recrystallisation

flow curves for C–Mn–Al steels. Materials Science and Technology. 1991;7(10):904-13.

15. Mintz B, Abushosha R, Jonas JJ. Influence of Dynamic Recrystallisation on the Tensile Ductility of Steels in the Temperature Range 700 to 1150.DEG.C. ISIJ International. 1992;32(2):241-9.

16. Ueki M, Horie S, Nakamura T. Factors affecting dynamic recrystallization of metals and alloys. Materials Science and Technology. 1987;3(5):329-37.

17. El-Meligy M, El-Bitar T, Ebied S. Creation of Fine Lath Martensite combined with Nano needle like Structured Carbides in Ultra high strength (UHS) Military Steel. Journal of Ultrafine Grained and Nanostructured Materials (JUFGNSM). 2023; 56 (2): 173-183.doi.10.22059/ JUFGNSM.2023.365577. 417.

18. Yue S. The Mathematical Modelling of Hot Rolling of Steel. Metal Forming Science and Practice: Elsevier; 2002. p. 213-26.

19. Cho S-H, Kang K-B, Jonas JJ. The Dynamic, Static and Metadynamic Recrystallization of a Nb-microalloyed Steel. ISIJ International. 2001;41(1):63-9.

20. Webb T.O, Van Aken D.C, Lekakh S.N. Evaluating Chemical Homogeneity in the Performance of Eglin Steel. 118th Annual Metal casting Congress ; 2014 April 8-11: Schaumburg, Illinois.

21. Webb T. O. Metallurgical optimization of high strength cast steels with stage I tempering. PhD Thesis, Missouri University of Science and Technology,USA; 2015.

22. Ren F, Chen F, Chen J. Investigation on Dynamic Recrystallization Behavior of Martensitic Stainless Steel. Advances in Materials Science and Engineering. 2014;2014:1-16.

23. Gruber C, Raninger P, Stanojevic A, Godor F, Rath M, Kozeschnik E, Stockinger M. Simulation of Dynamic and Meta-Dynamic Recrystallization Behavior of Forged Alloy 718 Parts Using a Multi-Class Grain Size Model. Materials (Basel). 2020;14(1):111.

24. Li H, Li X, Yan H, Li Y, Geng L, Xun C, et al. Constitutive Analysis and Microstructure Characteristics of As-Homogenized 2198 Al-Li Alloy under Different Hot Compression Deformation Conditions. Materials (Basel). 2023;16(7):2660.

25. Razali MK, Irani M, Joun M. General modeling of flow stress curves of alloys at elevated temperatures using bi-linearly interpolated or closed-form functions for material parameters. Journal of Materials Research and Technology. 2019;8(3):2710-20.